European Journal of Neuroscience, Vol. 12, pp. 2757–2768, 2000

Generation and propagation of 4-AP-induced epileptiform activity in neonatal intact limbic structures *in vitro*

H. J. Luhmann, V. I. Dzhala[1] and Y. Ben-Ari[1]
Institute of Neurophysiology, University of Duesseldorf, POB 101007, D-40001 Duesseldorf, Germany
[1]INMED, INSERM U29, Avenue de Luminy, B.P. 13 13273 Marseille Cedex 09, France

Keywords: 4-aminopyridine, development, entorhinal cortex, glutamate receptors, hippocampus, rat, seizures

Abstract

We examined the generation, propagation and pharmacology of 4-aminopyridine (4-AP)-induced epileptiform activity (EA) in the intact interconnected limbic structure of the newborn (P0–7) rat *in vitro*. Whole-cell recordings of CA3 pyramidal cells and multisite field potential recordings in CA3, CA1, dentate gyrus, and lateral and medial entorhinal cortex revealed 4-AP-induced EA as early as P0–1. At this age, EA was initiated in the CA3 region and propagated to CA1, but not to the entorhinal cortex. Starting from P3–4, EA propagated from CA3 to the entorhinal cortex. Along the CA3 septo-temporal axis, EA arose predominantly from the septal pole and spread towards the temporal site. Whereas the onset of 4-AP-induced EA decreased with age from 21.2 ± 1.6 min at P0–1 to 4.7 ± 0.63 min at P6–7, the seizure duration increased in the same age groups from 98 ± 14 s to 269.4 ± 85.9 s, respectively. The EA was blocked by 6-cyano-7-nitroquinoxaline-2,3-dione (CNQX) but not by DL-2-amino-5-phosphonovaleric acid (APV), (+)-MK-801 hydrogen maleate (MK-801) or (±)-alpha-methyl-4-carboxyphenylglycine (MCPG), suggesting that they were mediated by α-amino-3-hydroxy-5-methyl-4-isoxazolepropionate (AMPA)/kainate receptor activation. We conclude that: (i) the septal pole of the hippocampal CA3 region plays a central role in the generation of EA in the neonatal limbic system; and (ii) AMPA/kainate receptor-mediated EA can be generated in CA3 already at birth. Therefore, the recurrent collateral synapses and circuits required for the generation of EA are developed earlier than previously suggested on the basis of studies on hippocampal slices.

Introduction

Besides its central role in memory acquisition, the entorhinal cortex–hippocampal formation is clearly involved in the generation and amplification of epileptic seizures (for review, see Lothman *et al*., 1991). About 80% of the pharmaco-resistant epilepsy arises from the temporal lobe, reinforcing the function of the entorhinal cortex and the hippocampus in this pathophysiological condition. Despite numerous studies on 'seizure circuits in the hippocampus and associated structures' (Lothman, 1994), the exact role of these two structures in the generation of epileptic activity is not completely understood (for review, see Heinemann *et al*., 1993). In some conditions, seizures originate in the entorhinal cortex and propagate via the dentate gyrus to the hippocampus proper from where they may re-enter the entorhinal cortex (for review, see Jones, 1993), in other conditions the CA3 region may act as the 'pacemaker' and subsequently activates area CA1 and the entorhinal cortex (for review, see Lothman, 1994).

An understanding of the mechanisms underlying seizure generation and propagation is extremely important in the immature brain, because epilepsy is a common neurological disorder in children (for review, see Aicardi, 1986), and seizures in the developing brain may induce long-term deficits (for review, see Holmes & Ben-Ari, 1998). However, the experimental analysis of this question is difficult, because electrophysiological recordings in *in vivo* and whole-brain *in vitro* preparations are more difficult to perform in the immature brain.

Correspondence: Dr H. J. Luhmann, as above.
E-mail: luhmann@uni-duesseldorf.de

Received 30 December 1999, revised 10 April 2000, accepted 19 April 2000

We used a new *in vitro* preparation of the intact hippocampal formation (IHF) with preserved connectivity to the entorhinal cortex (Khalilov *et al*., 1997) to study in the neonatal rat the following questions: (i) which structures are prone to epileptiform activity (EA) in the immature hippocampal–entorhinal complex; (ii) which routes of seizure propagation are realized at this age; and (iii) which glutamate receptors are involved in this activity? We used the 4-aminopyridine (4-AP) model (Perreault & Avoli, 1989; Avoli *et al*., 1993) to induce EA in the intact hippocampus–entorhinal cortex *in vitro*.

Some of the results have been presented in abstract form (Luhmann *et al*., 1998).

Materials and methods

Tissue preparation

The methods for preparing the intact hippocampus–entorhinal cortex were similar to those described previously for the intact hippocampus *in vitro* preparation (Khalilov *et al*., 1997). Neonatal Wistar rats [postnatal day (P) 0–7; day of birth = P0] were deeply anaesthetized by hypothermia and decapitated. The brain was rapidly removed and transferred to oxygenated (95% O_2/5% CO_2) ice-cold (2–5 °C) artificial cerebrospinal fluid (ACSF) of the following composition (in mM): NaCl, 126; KCl, 3.5; $CaCl_2$, 2.0; $MgCl_2$, 2.0; $NaHCO_3$, 25; NaH_2PO_4, 1.2; glucose, 11; pH 7.4. The subsequent preparation of the intact hippocampus–entorhinal cortex was performed in oxygenated ice-cold ACSF. Intact hippocampi were dissected and transferred to a beaker containing oxygenated ACSF and kept there at room temperature (20–22 °C) for at least 2 h before use. For recordings,

the tissue was placed into a conventional fully submerged chamber superfused with ACSF at 32–33 °C at a rate of 8–10 mL/min. The hippocampi were placed on the plastic mesh by the ventral side down allowing an easy access to the CA3 and CA1 regions. Then the hippocampi were fixed to the silgard bottom using several entomological needles.

Whole-cell recordings, multisite extracellular recordings and data analysis

Whole-cell recordings were performed in the CA3 area using an Axopatch 200A (Axon Instruments, Foster City, CA, USA) amplifier. Patch electrodes were made from borosilicate glass capillaries (outside diameter 1.5 mm, inside diameter 0.86 mm; type GC150F-15, Clark Electromedical Instruments, Pangbourne, England), and had an input resistance of 6–8 MΩ when filled with solution containing (in mM): K-gluconate, 135; $CaCl_2$, 0.1; $MgCl_2$, 2; Na_2ATP, 2; ethylene glycol-bis (b-aminoethyl ether)-*N*,*N*,*N*′,*N*′-tetraacetic acid (EGTA), 1; *N*-2-hydroxyethylpiperazine-*N*-2-ethane-sulphonic acid (HEPES), 10; pH 7.25; osmolarity 280 mOsm. After dialysis with this solution, $GABA_A$ (γ-aminobutyric acid) receptor-mediated synaptic currents reversed at ~–64 mV. Putative CA3 pyramidal cells were recorded in the pyramidal cell layer, which can be seen as a light band in a transluminescent microscope. The cellular type of the recorded neurons was identified based on the action potential and accommodation properties. Simultaneous extracellular field potentials were recorded in the stratum radiatum of the CA3 subfield with a glass microelectrode (1.2 mm outside diameter and 0.94 mm inside diameter; GC120TF-10, Clark Electromedical Instruments) filled with ACSF and connected to a DAM-80C AC differential amplifier (World Precision Instruments, USA). Tungsten bipolar electrodes disposed in the stratum radiatum of CA3 area were used to evoke synaptic responses. The stimulation parameters were 20–30 V in amplitude and 20 μs in duration. Whole-cell and simultaneous extracellular recordings were acquired into the memory of a Pentium-II personal computer using an Digidata-1200 analogue-to-digital converter (Axon Instruments). Axotape 7.0 (Axon Instruments), Acquis (Gerard Sadoc, France) and Origin 5.0 (Microcal Software, Northampton, MA, USA) programs were used for the acquisition and analysis of the synaptic activities.

Extracellular multisite recordings were performed with five tungsten 4–5 MΩ microelectrodes (FHC, Brunswick, USA) positioned in area CA3, area CA1, dentate gyrus, lateral and medial entorhinal cortex. Signals were AC recorded with extracellular amplifiers, low-pass filtered at 3 kHz, stored and analysed with an eight-channel PC-based software program (TIDA, Heka, Lambrecht, Germany). An eight-channel chart recorder (MT95000, Astromed, Rodgau, Germany) was used to visualize the signals on-line. 4-Aminopyridine (Sigma, Deisenhofen, Germany) was added to the bathing solution at a concentration of 50–100 μM (Perreault & Avoli, 1989). The 4-AP-induced spontaneous epileptiform events were analysed in their duration, onset latency and amplitude by measuring in extracellular recordings the voltage between the positive- and negative-going peak. The propagation of epileptiform events was analysed by setting the time point of the earliest visible deflection of all five recording sites to 0 ms and by measuring the time delay to the response in the remaining field potential recordings. The average data from these measurements were used to construct a scheme for the propagation of epileptiform activity between the five recording sites (Fig. 5D, E and I).

The non-specific metabotropic glutamate antagonist (±)-alpha-methyl-4-carboxyphenylglycine (MCPG, RBI, Natick, MA, USA; 500 μM), the competitive *N*-methyl-D-aspartate (NMDA) antagonist DL-2-amino-5-phosphonovaleric acid (APV, Sigma; 30–60 μM), the non-competitive NMDA antagonist (+)-MK-801 hydrogen maleate (MK-801, RBI; 10–20 μM) and the α-amino-3-hydroxy-5-methyl-4-isoxazolepropionic (AMPA)/kainate antagonist 6-cyano-7-nitroquinoxaline-2,3-dione (CNQX, RBI; 5–10 μM) were bath-applied and washed in for at least 20 min before further analysis.

Values throughout this report are given as mean ± SEM. For statistical analyses, a Mann–Whitney *U*-test or Student's *t*-test, was performed. Statistical significance of differences was assessed with the level of significance set at $P < 0.05$.

Results

4-AP effects in area CA3 of the intact hippocampus of the neonatal rat

Simultaneous whole-cell current-clamp recordings of CA3 pyramidal cells and extracellular field potential recordings in CA3 stratum radiatum were performed to analyse the effects of 4-AP in the P4–5 intact hippocampus (Fig. 1). 4-AP caused a prominent increase in the duration of the action potential due to a slower repolarization phase (insert in Fig. 1A). Interictal events occurred synchronously in the whole-cell and extracellular recording (Fig. 1A, B1 and C1) and were followed by the ictal phase consisting of the tonic (Fig. 1B2 and C2) and clonic components (Fig. 1B3 and C3). During the ictal tonic phase, the membrane depolarized to ~–20 mV and gradually recovered within 2–3 min of the ictal clonic phase to the control value of –63.9 ± 2.2 mV ($n = 6$, resting membrane potential in control). The ictal discharge was followed by a post-ictal depression with reduced synaptic activity and a hyperpolarization to –68.7 ± 2.1 mV ($n = 6$, Fig. 1A). Therefore, EA can be generated in the intact preparation by 4-AP with all the phases that are observed *in vivo*.

4-AP also caused a prominent increase in the frequency of spontaneous network-driven giant depolarizing potentials (GDPs), which can be observed in the rat hippocampus during the first postnatal week (Ben-Ari *et al.*, 1989). Already at P0–1, under control conditions in normal bathing solution, simultaneous whole-cell voltage-clamp recordings of CA3 pyramidal cells and extracellular field potential recordings in CA3 stratum radiatum revealed GDPs with an average frequency of 1.1–0.26 min^{-1} ($n = 6$ hippocampi, outward currents in upper trace of Fig. 2A and B, Ben-Ari *et al.*, 1989; Khazipov *et al.*, 1997). Bath application of 100 μM 4-AP for > 5 min induced a gradual increase in the frequency of GDPs up to 5.7 ± 0.45 min^{-1} and a rise in the frequency of spontaneous postsynaptic currents (Fig. 2B), followed by a seizure-like discharge consisting of an interictal phase and ictal clonic components (Fig. 2A and C). The early ictal phase was characterized by large-amplitude (> 200 pA) and > 500 ms in duration polysynaptic bursts synchronous with population network activity in the field recording (Fig. 2C1). These bursts in the field potential recordings were characterized by oscillations in the gamma frequency range (~40 Hz) which were synchronous with glutamate-mediated postsynaptic currents recorded in the whole-cell mode. The early ictal activity was followed by a clonic phase lasting up to 98 ± 24 s ($n = 6$) and characterized by repetitive inward currents of ~ 100 pA in amplitude and with a slowly decreasing frequency from 2 to 0.125 Hz. These data demonstrate that already the hippocampus of the newborn (P0–1) rat is capable of generating seizure-like activity *in vitro*.

Developmental profile of 4-AP-induced epileptiform activity

The expression and propagation pattern of 4-AP-induced EA was strongly age dependent. In the intact hippocampus prepared from

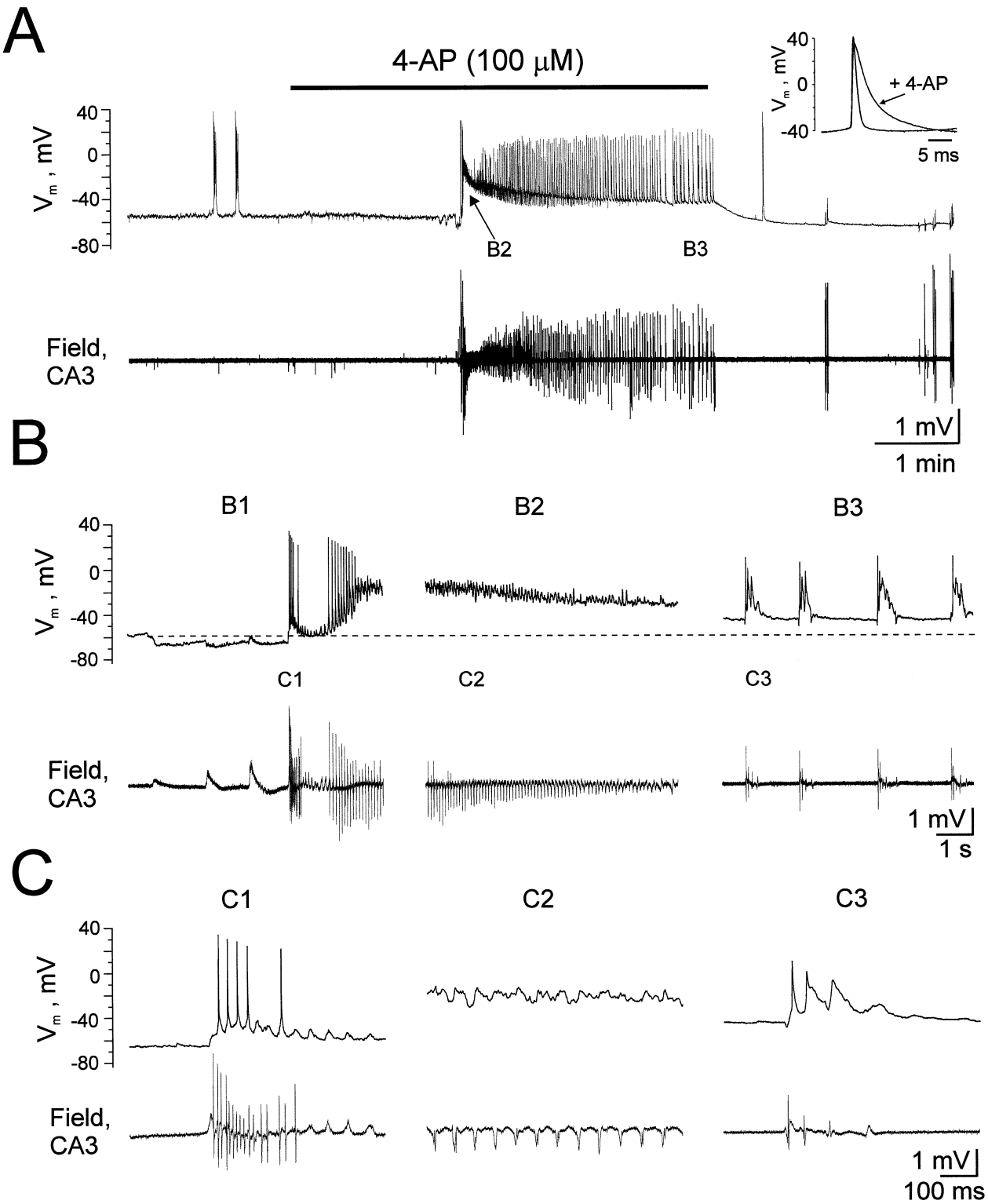

FIG. 1. Effects of 100 μM 4-AP on neuronal activity and induction of epileptiform activity in the intact hippocampus *in vitro* preparation of a P4 rat. (A) Simultaneous recordings in whole-cell current-clamp configuration of a CA3 pyramidal cell (upper trace) and extracellular field potential (lower trace) in the stratum radiatum layer of the CA3 area. Insertion shows prominent increase in action potential duration due to slow repolarization phase. (B and C) Phases of the ictal activity on an expanded time scale.

P0–1 rats, perfusion of 100 μM 4-AP elicited in area CA3 after 21.2 ± 1.6 min ($n = 6$) interictal and ictal tonic–clonic discharges in 100% and 16.6% of the cases, respectively (Fig. 3A and B). Ictal discharges lasted for 98 ± 14 s and were observed synchronously in the whole-cell and field potential recordings. In the P2–3 intact hippocampus, ictal tonic–clonic discharges could be observed in 50% of the cases ($n = 6$), appeared after 14.8 ± 1.2 min of 4-AP perfusion and lasted 121 ± 14.6 s ($n = 6$, Fig. 3). The 4-AP-induced seizure

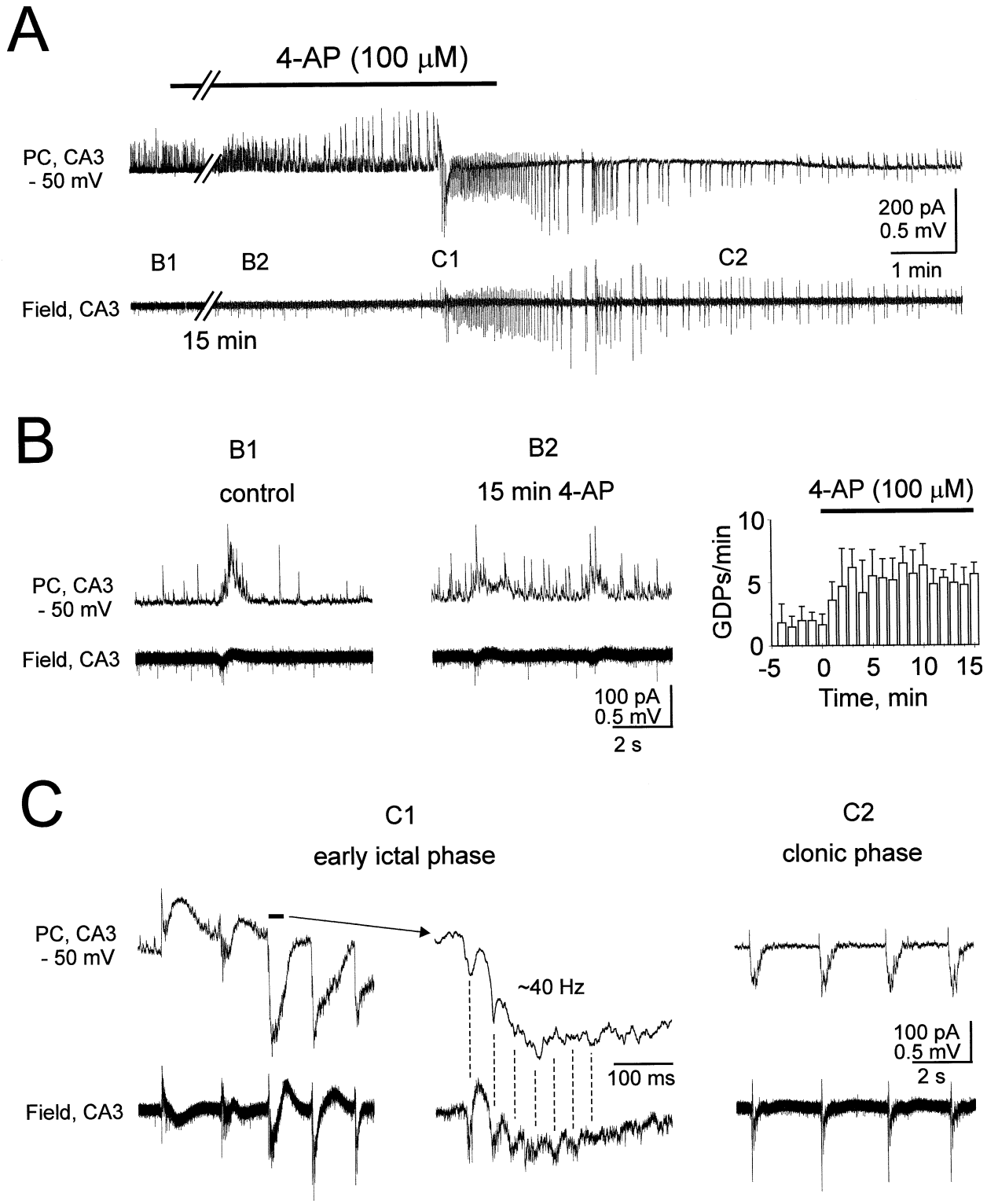

FIG. 2. Effects of 4-AP on network-driven activity and expression of epileptiform activity in the intact hippocampus of a P1 rat. Simultaneous whole-cell recording of a CA3 pyramidal cell (upper traces) and extracellular field potential (lower traces) in stratum radiatum of area CA3. The CA3 pyramidal cell was recorded in whole-cell voltage-clamp configuration at –50 mV so that GABAergic currents are outwardly and glutamatergic currents are inwardly directed. (A) Bath application of 100 μM 4-AP causes a transient increase in the frequency of GDPs and spontaneous postsynaptic currents followed by an ictal discharge. (B) Parts of traces from A on an expanded time scale showing increased GDP frequency during 4-AP application. Diagram of GDPs frequency in control conditions and during 4-AP application ($n = 6$). (C) Early ictal phase and clonic phase of the epileptiform activity on an expanded time scale (see time points in A). Field potential recording of early ictal phase shows gamma frequency oscillation (~40 Hz) that is synchronous with glutamate-mediated postsynaptic currents.

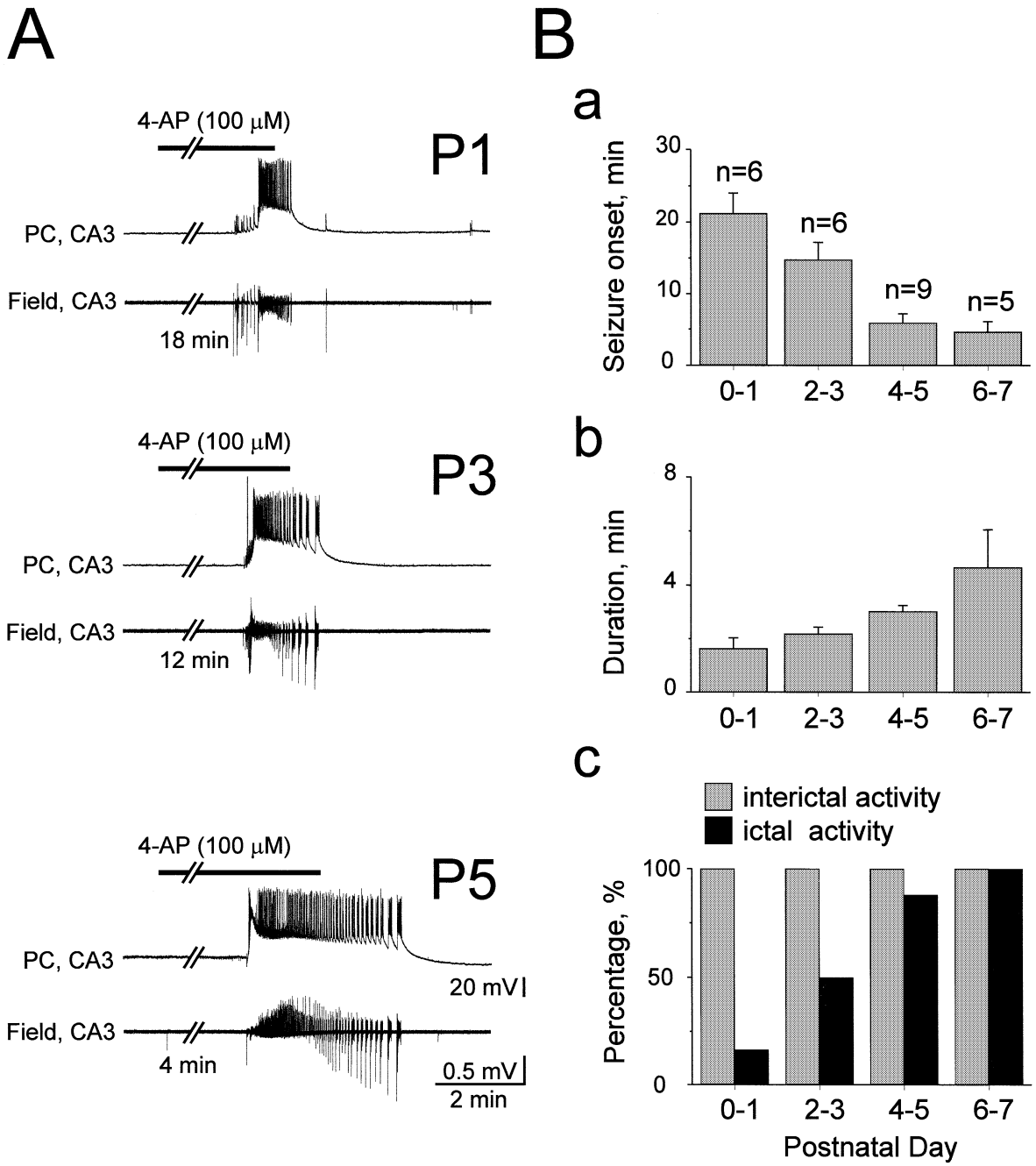

FIG. 3. Developmental profile of the epileptogenic effect of 4-AP in the intact hippocampus of the P0–7 rat. (A) Simultaneous recordings of the CA3 pyramidal cell in whole-cell current-clamp mode (upper trace) and extracellular field potentials in stratum radiatum of area CA3. Note age-dependent decrease of seizure onset after 4-AP application and increase in duration. (B) Diagrams of average seizure onset (a), duration of ictal discharge (b) and the percentage of cases (c) in which 4-AP induced interictal activity (shaded columns) and ictal activity (black columns). Numbers in (Ba) indicate number of hippocampi per age group. Data in B are expressed as mean ± SEM.

onset showed a further decrease with maturation of the neuronal network. In the P4–5 hippocampus, ictal tonic–clonic activity of 174 ± 4.9 s in duration already emerged after 5.9 ± 0.46 min of 4-AP perfusion and could be observed in 88% of the cases ($n = 9$, Fig. 3). Finally, in the P6–7 intact hippocampus, ictal tonic–clonic discharges were generated after 4.7 ± 0.63 min of 4-AP application in 100% of the cases ($n = 5$). In this age group, the ictal discharges consisting of the characteristic tonic and clonic phase showed the longest duration (269.4 ± 85.9 s, Fig. 3). Therefore, EA can be generated early in postnatal hippocampi.

4-AP-induced long-lasting modifications in neuronal activity

The long-lasting epileptogenic action of 4-AP was studied during persistent (up to 8 h) bath application of 100 μM 4-AP. After 20–40 min of 4-AP application, a very regular and spontaneous seizure-like discharge pattern developed, which could be recorded consistently for hours in area CA3 with extracellular electrodes (Fig. 4A). The interval between ictal discharges varied from 6 to 15 min in different experiments. Interictal events of 366 ± 35 μV ($n = 33$) in amplitude and 193 ± 13 ms in duration could be observed at intervals

of 2–8 s (Fig. 4B and C). These interictal events triggered the ictal activity consisting of the tonic (Fig. 4B and D) and clonic component (Fig. 4B and E). The first collective spike of the ictal tonic phase amounted to 690 ± 85 μV ($n = 15$) in amplitude and was followed by a barrage of ~ 10 Hz rhythmic spikes which gradually transposed into ictal clonic activity (Fig. 4B and D). Clonic activity recorded in the CA3 region consisted of double or triple spikes occurring every 0.5–2 s, measuring 376 ± 24 μV ($n = 32$) in amplitude and lasting 363 ± 27 ms (Fig. 4B and E). Therefore, a persistent pattern of EA can be recorded with long-lasting applications of 4AP.

Initiation and propagation of epileptiform activity in the intact hippocampus–entorhinal cortex

The initiation and propagation of 4-AP-induced spontaneous EA was studied in the intact hippocampus connected to the entorhinal cortex with five extracellular electrodes positioned in area CA3, area CA1, dentate gyrus, lateral and medial entorhinal cortex (Fig. 5). In agreement with previous studies in adult mice (Barbarosie & Avoli, 1997) and adult rats (Avoli *et al*., 1996), our quantitative analyses in rats older than P2 demonstrated that interictal activity is initiated in

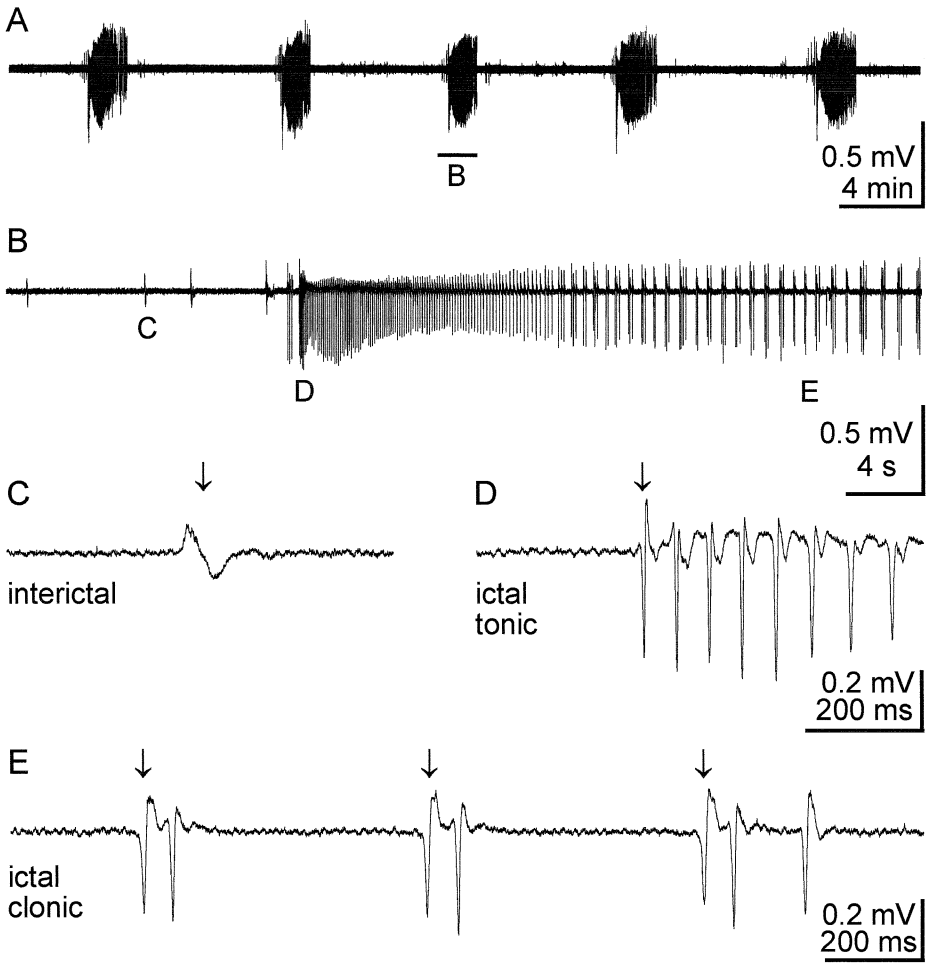

FIG. 4. Extracellular recording of spontaneous epileptiform activity in the CA3 region of the intact hippocampus–entorhinal cortex preparation of a P6 rat during persistent 4-AP application (> 2 h). (A) Five ictal events occurring at intervals of 8–10 min. The middle event is shown at higher temporal resolution in B. (B) Small interictal events (C), early ictal tonic activity (D) and ictal clonic activity (E). (C–E) Downward arrows mark interictal (C), ictal tonic (D) and ictal clonic (E) events, which were selected for quantitative analyses.

FIG. 5. Spread of epileptiform activity in the intact hippocampus–entorhinal cortex preparation of a P5 (A–E) and P0 (F–I) rat. The five extracellular recording electrodes were located in area CA3, area CA1, lateral entorhinal cortex, medial entorhinal cortex and dentate gyrus (from upper to bottom trace in A–C). (A–C) Simultaneous recordings of interictal (A), ictal tonic (B) and ictal clonic (C) events in P5 rat. Vertical dotted lines mark beginning of activity at the five recording sites. Note propagation of interictal and ictal clonic activity from CA3 to other regions. (D and E) Schematic illustration of propagation pattern of interictal (D) and ictal clonic activity (E). (F–H) 4-AP-induced epileptiform activity in the P0 rat is generated in the CA3 region and does not spread to the entorhinal cortex or dentate gyrus. Note small CA1 response in H. Time points of traces in G and H are indicated in F. (I) Schematic illustration of propagation pattern of 4-AP-induced epileptiform events in the P0 preparation. Length of arrows in D, E and I indicate average time delays of the onset for the epileptiform events (see 15 ms arrow for scaling). Dotted arrows in D and E indicate alternative route of activation. (J) Average amplitude of epileptiform events recorded in the CA3 (shaded) and CA1 (black) region of P5–6 rats (interictal, $n = 26$; ictal tonic, $n = 12$; ictal clonic, $n = 21$) and P0 rats ($n = 24$).

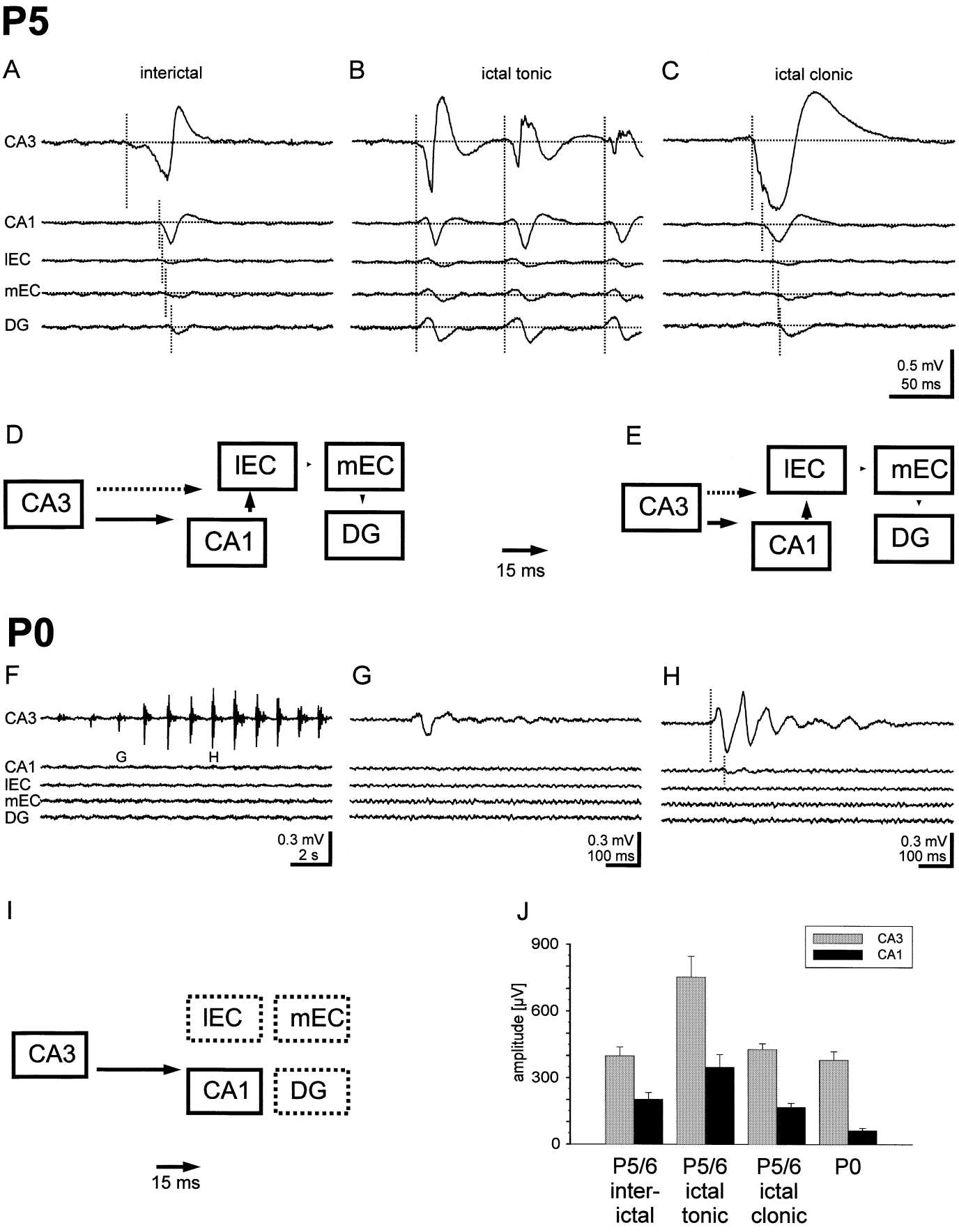
P5
A
interictal
B
ictal tonic
C
ictal clonic
CA3
CA1
lEC
mEC
DG
0.5 mV
50 ms
D
CA3
lEC
mEC
CA1
DG
15 ms
E
CA3
lEC
mEC
CA1
DG
P0
F
G
H
CA3
G
H
CA1
lEC
mEC
DG
0.3 mV
2 s
0.3 mV
100 ms
0.3 mV
100 ms
I
CA3
lEC
mEC
CA1
DG
15 ms
J
CA3
CA1
amplitude [μV]
900
600
300
0
P5/6 inter-ictal
P5/6 ictal tonic
P5/6 ictal clonic
P0

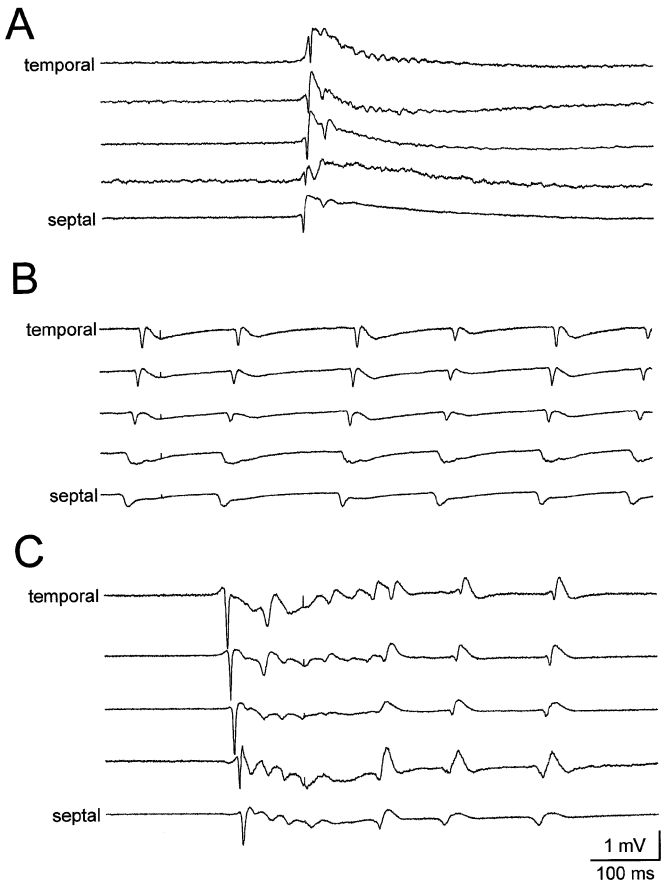

FIG. 6. 4-AP-induced epileptiform events in the CA3 region are initiated at different locations of the P6 intact hippocampus. The five recording electrodes were positioned in the CA3 region along the longitudinal axis from the temporal (upper trace) to the septal pole (lower trace). Whereas interictal bursts (A) and ictal tonic discharges (B) were predominantly generated at the septal pole, ictal clonic events (C) arose either from the temporal or septal pole.

the CA3 region (Fig. 5A). After an average delay of 25.5 ± 3.7 ms ($n = 8$), interictal 185 ± 26 μV ($n = 33$) large events can be observed in the CA1 region (Fig. 5A and D). From area CA1 the activity propagates (directly or via the subiculum) with a delay of 7.1 ± 1.9 ms ($n = 7$) to the lateral entorhinal cortex, where the average field potential amplitudes amounted to only 9 ± 3 μV ($n = 24$, Fig. 5A and D). Because epileptiform activity arising in the CA3 subfield may be transferred to the entorhinal cortex (for review, see Jones, 1993), interictal events originating in CA3 may also directly propagate to the lateral entorhinal cortex with a delay of 34.4 ± 4 ms (Fig. 5D). From the lateral entorhinal cortex, interictal events spread with a delay of 1.3 ± 0.9 ms to the medial entorhinal cortex (16 ± 3 μV) and finally, during high-frequency discharge (for review, see Jones, 1993) and after a further delay of 3.1 ± 1.3 ms, to the dentate gyrus (46 ± 5 μV, $n = 33$). We have no evidence for a re-entry of interictal activity from the dentate gyrus into the CA3 region in the age group studied (Fig. 5A and D). In contrast to the interictal events, ictal tonic activity occurred almost simultaneously at all five recording sites (Fig. 5B). Again, the largest amplitudes could be observed in the CA3 (690 ± 85 μV, $n = 15$) and in the CA1 subfield (321 ± 48 μV, $n = 15$), and smaller ictal events were recorded in the lateral entorhinal cortex (27 ± 8 μV, $n = 12$), medial entorhinal cortex (55 ± 6 μV, $n = 15$) and in the dentate gyrus (118 ± 17 μV, $n = 15$, Fig. 5B). Ictal clonic events with an average amplitude of 376 ± 24 μV ($n = 32$) were initiated in the CA3 region, from where they propagated with a delay of 9.9 ± 0.8 ms to the CA1 subfield (148 ± 16 μV, $n = 32$, Fig. 5C and E). These CA1 ictal clonic events arrive in the lateral entorhinal cortex (28 ± 26 μV, $n = 32$) after a delay of 6.3 ± 1.5 ms or may be transferred directly from the CA3 area with a delay of 16.1 ± 1.6 ms. From the lateral entorhinal cortex, ictal clonic events propagated with a delay of 1.8 ± 1.2 ms to the medial entorhinal cortex (61.3 ± 4.2 μV, $n = 32$) and from there after 1.8 ± 0.7 ms to the dentate gyrus (113 ± 11 μV, $n = 32$, Fig. 5C and E).

Whereas in P3–6 rats, epileptiform events could be consistently recorded at all five recording sites, 4-AP application in P0 rats elicited EA, that was predominantly restricted to the CA3 region (Fig. 5F–I). Interictal-like events occurring every ~2 s in CA3 gradually increased in amplitude to a maximum of 380 ± 39 μV ($n = 24$, Fig. 5F and G). These relatively large events were followed by four to six waves of smaller amplitude and propagated to the CA1 subfield, where they amounted to 61 ± 12 μV ($n = 24$) in amplitude (Fig. 5H). We have never observed a propagation to the entorhinal cortex or dentate gyrus, indicating that at P0 the 4-AP-induced epileptiform events are initiated in CA3 and only spread to the CA1 region (Fig. 5I). The average amplitude of the EA recorded in the CA3 region of the P0 rat is in the range of the amplitude of the interictal and ictal clonic events observed in the P5–6 rat (Fig. 5J), indicating that the absence of spread in the P0 hippocampus–entorhinal cortex is not due to decreased excitation in CA3.

In order to address the question, which pole of the intact hippocampus may trigger the 4-AP-induced EA, we positioned five extracellular electrodes along the longitudinal axis from the temporal to the septal pole in the CA3 area of the hippocampus (Fig. 6). This experimental approach demonstrated that interictal bursts and ictal tonic discharges were generally initiated at the more septal pole (Fig. 6A and B), whereas ictal clonic events arose either from the septal or temporal pole (Fig. 6C). These data suggest that EA may be initiated at different locations of the CA3 region in the P3–6 hippocampus with predominance of a septo-temporal vector in their propagation.

Influence of glutamate antagonists on 4-AP-induced epileptiform activity

The effects of metabotropic and ionotropic glutamate antagonists on the initiation and propagation of 4-AP-induced EA were studied in intact hippocampus–entorhinal cortex preparations from P3–6 rats with multisite extracellular recordings. Under control conditions in 4-AP containing ACSF, interictal, ictal tonic and ictal clonic events consistently showed the largest amplitude in the CA3 region (Fig. 5A–C). The non-selective metabotropic glutamate antagonist MCPG (500 μM) did not significantly (all $P > 0.2$) affect the amplitude or the spread of interictal ($n = 7$), ictal tonic ($n = 4$) or ictal clonic ($n = 21$) activity (Fig. 7A–C). Similar results could be obtained with the competitive NMDA antagonist APV (30–60 μM), which had no significant (all $P > 0.07$) influence on the amplitude of the interictal ($n = 13$), ictal tonic ($n = 5$) or ictal clonic ($n = 7$) events (Fig. 7D–F). The non-competitive NMDA antagonist MK-801 (10–20 μM) caused in the CA1 region a significant ($P = 0.049$, $n = 10$) increase in the amplitude of the interictal activity (Fig. 7G). All other interictal ($n = 10$), ictal tonic ($n = 5$) and ictal clonic ($n = 12$) events were not significantly (all $P > 0.09$) affected by MK-801 (Fig. 7G–I). In contrast, the AMPA/kainate antagonist CNQX (5–10 μM) blocked in all cases ($n = 4$) the interictal, ictal tonic and ictal clonic events (Fig. 7J–L). This effect was reversible after washout of CNQX. Therefore, glutamatergic EA can be recorded already at birth.

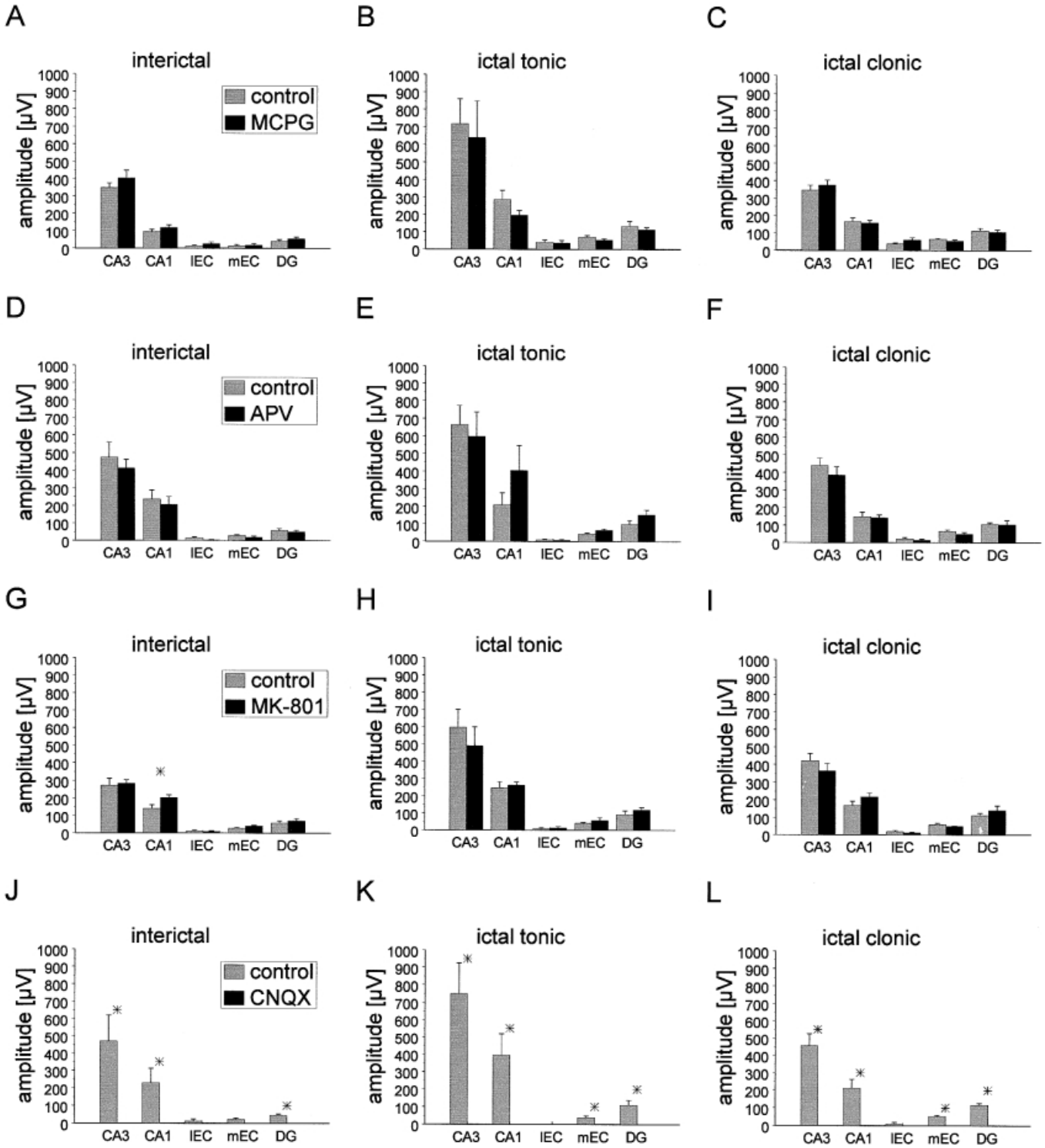

FIG. 7. Effects of glutamate antagonists on the amplitude of 4-AP-induced interictal, ictal tonic and ictal clonic activity recorded simultaneously in CA3, CA1, lateral and medial entorhinal cortex, and dentate gyrus of P3–6 rats. Control data are presented in shaded bars. (A–C) Effects of the non-specific metabotropic glutamate antagonist MCPG (500 μM). (D–F) Influence of the competitive NMDA antagonist APV (30–60 μM). (G–I) Effects of the non-competitive NMDA antagonist MK-801 (10–20 μM). (J–L) Blockade of all epileptiform activity by the AMPA/kainate antagonist CNQX (5–10 μM). Data are expressed as mean ± SEM. Statistical significant differences at the $P < 0.05$ level are indicated by an asterisk.

Discussion

In this study we used the *in vitro* preparation of the IHF with preserved connectivity to the entorhinal cortex (Khalilov *et al*., 1997) to analyse the generation, propagation and pharmacology of 4-AP-induced EA in the neonatal rat. The main results of these experiments are as follows. (i) EA can be reliably recorded for 6–8 h in this preparation. (ii) EA originating in CA3 and propagating to CA1 can be already observed in P0 rats. (iii) In P4–6 rats, interictal discharges recorded in CA3 pyramidal cells coincide with field potentials in CA3

stratum radiatum and spread via CA1 to the entorhinal cortex and dentate gyrus. Within CA3, interictal activity arose from the septal pole. (iv) Ictal tonic discharges occur almost synchronously in the hippocampal formation and entorhinal cortex. (v) EA can be blocked by an AMPA/kainate receptor antagonist, but not by antagonists acting at the NMDA or metabotropic glutamate receptor.

Area CA3 as pacemaker in the neonatal limbic system

Our data clearly indicate that the CA3 region, especially the septal pole, acts as the primary initiation site for the generation of EA in the limbic system of the neonatal rat. The CA3 region also consistently revealed the largest amplitude for the three different types of spontaneous 4-AP-induced EA, supporting the crucial role of this area in seizure initiation during this developmental period. The concurrent expression of EA at the single-cell level and in the field potential recordings indicates that CA3 pyramidal neurons form an excitatory network as early as P0–1.

In contrast to previous studies on hippocampal slices (Swann & Brady, 1984; Gomez-Di Cesare *et al*., 1997), our data demonstrate that the CA3 network is capable of generating full interictal and ictal tonic–clonic discharges already in the newborn rat. Similar observations have been recently made using the same intact preparation and studying kainate-induced EA. Interictal activities were readily observed at P1–2 and ictal discharges as early as P3–4 (Khalilov *et al*., 1999). This discrepancy probably results from a loss of long-range axonal projections during the slicing procedure, because previous *in vivo* experiments have demonstrated kainate-induced seizures starting from P4–5 (Cherubini *et al*., 1983), and using 2-deoxyglucose autoradiography, Tremblay *et al*. (1984) reported enhanced activity restricted to the CA3 region as early as P2. These observations emphasize the relevance of the intact preparations at an early developmental stage – at a time when the density of synapses is small – because the destruction by the slicing procedure of a significant proportion of neuronal connections may be particularly deleterious for the study of polysynaptic activities.

Our observation on the propensity of the septal (dorsal) pole in generating epileptiform discharges in the neonatal CA3 region is in disagreement with previous studies in mature animals. Paré *et al*. (1992) demonstrated in the isolated brain *in vitro* preparation of the adult guinea pig a greater propensity of the temporal (ventral) hippocampus and a spread of EA to the septal site. Similar results have been reported by Lee *et al*. (1990) for rat hippocampal slices. In contrast, using the rat IHF preparation, both giant depolarizing potentials (Leinekugel *et al*., 1998) and kainate-induced seizures (Khalilov *et al*., 1999) show a similar propensity for a septo-temporal propagation. Furthermore, preliminary studies using the low-magnesium epilepsy model (unpublished observations) also indicate that the septal region initiates the EA in area CA3 of the neonatal rat IHF.

The preservation of axonal connections in the IHF does not only promote the network activity within the CA3 region, but also facilitates the propagation of EA to other areas of the limbic system. Previous studies in conventional hippocampal slices from mature guinea pigs (Schwartzkroin & Prince, 1978), in combined hippocampal–entorhinal cortex slices from adult mouse (Barbarosie & Avoli, 1997), and in the isolated adult guinea pig brain (Paré *et al*., 1992) have already shown that interictal discharges arise in the CA3 region and propagate via Schaffer collaterals to the CA1 area. Our observations clearly demonstrate that this connection reliably transfers interictal and ictal clonic activity from CA3 to CA1 already in the P4–5 rat. In the rat, CA3 pyramidal neurons are generated on embryonic day 17–18 (Bayer, 1980), and Morest (1970) suggested that hippocampal pyramidal cells already project to other brain regions before migrating to their final positions. An early morphological (Supèr & Soriano, 1994) and physiological (Diabira *et al*., 1999) development of the Schaffer collaterals has been reported. An early development of the hippocampal-septal projection, preceding the septo-hippocampal projection, has been described by Linke & Frotscher (1993) in the rat. Because the Schaffer collateral system 'possesses a hitherto unappreciated order and widespread distribution' (Witter, 1993), the IHF represents the ideal preparation to study the function of this early projection *in vitro*. In the neonatal rat, area CA3 may activate the entorhinal cortex via a direct projection (Swanson & Cowan, 1977) or indirectly via area CA1 (Witter, 1993), either diffusely, causing an almost simultaneous activation of the lateral and medial areas, or initially exciting the lateral entorhinal cortex followed by the medial part (Iijima *et al*., 1996).

Our data obtained in the P5–6 rat intact hippocampus are fully compatible with this sequence of activation in the limbic system, supporting the 'pacemaker' role of the CA3 region (for review, see Lothman, 1994). In none of our 4-AP experiments did we observe an initiation of EA in the entorhinal cortex, as reported in the adult rat (for review, see Heinemann *et al*., 1993; Jones, 1993). However, addition of bicuculline methiodide (10 μM) to the 4-AP-containing bathing solution may also cause an initiation of EA in the entorhinal cortex, suggesting that this brain region is capable of generating seizure activity in the neonatal limbic system (unpublished observations).

Interestingly, the CA3 region of the neonatal rat hippocampus does not only act as a pacemaker for EA, but is also capable of generating gamma oscillations in the frequency range of 40 Hz. Network oscillations at lower gamma frequencies (20–40 Hz) and high frequencies between 100 and 400 Hz have been recently described by Palva *et al*. (2000) in the P3–6 rat CA3 region in normal bathing solution. As in the retina and cerebral cortex, synchronized network oscillations may shape connectivity in the neonatal hippocampal network (for review, see Katz, 1993).

Different propagation patterns of ictal tonic and clonic activities

As in adult rats, the EA originating in the hippocampus and invading the entorhinal cortex are transferred via the perforant path to the dentate gyrus in P5–6 animals (for review, see Lothman, 1994). However, in contrast to the seizure spread in mature animals (Paré *et al*., 1992; Barbarosie & Avoli, 1997), we have no evidence for a re-entry of EA into the hippocampus via the dentate gyrus. It has been previously postulated that the dentate gyrus with its resistance to paroxysmal activity may operate as a brake or filter for these reverberatory seizures (for review, see Heinemann *et al*., 1993; Lothman, 1994). Our observations in the intact P0–6 rat hippocampus indicate that this brake, probably also attributed to the immaturity of the dentate gyrus, hinders the re-entry into the hippocampus via mossy fibres in the neonatal limbic system suggesting, in keeping with extensive *in vivo* studies (Tremblay *et al*., 1984), that the seizures will not activate the entire limbic system at this stage. The lack of re-entry of EA in the CA3 region has been suggested to underlie the lack of neuropathological consequences of seizures at this early developmental stage (Nitecka *et al*., 1984; for review, see Ben-Ari, 1987).

Although the full sequence of interictal, ictal tonic and ictal clonic activity followed by post-ictal depression could be observed already in the newborn rat hippocampus, there are differences in their propagation patterns. Interictal discharges as well as ictal clonic discharges originated in area CA3 and revealed a characteristic

propagation pattern that probably depends on the sequential maturation of axonal connections between this region and other limbic structures. These observations confirm the central role of CA3 as a pacemaker already in early postnatal life for the generation of EA. In adult rat hippocampal slices 4-AP-induced ictal discharges originate in the entorhinal cortex and are mediated by NMDA receptors (Avoli *et al*., 1996; for review, see Jones, 1993). Other studies suggest a propensity of the CA1 region to generate ictal events (for review, see Lothman, 1994). Finally, ictal tonic discharges occurred almost simultaneously at all recording sites in the neonatal limbic system, suggesting that different mechanisms underlie the generation and propagation of the various components of EA.

An early role for glutamate receptors in the generation of EA

The development of the hippocampal circuit is associated with a sequential expression of the main ionotropic receptors. Thus, GABAergic synapses are established first, probably on the dendrites of the principal cells (Tyzio *et al*., 1999), and exert an excitatory action due to a different chloride gradient (for review, see Ben-Ari *et al*., 1997). NMDA receptors are functional earlier than the main glutamate ionotropic receptor AMPA (Durand *et al*., 1996), and there are indications that the expression of the latter may be activity dependent requiring the prior activation of NMDA receptors (Isaac *et al*., 1995). In the present study, neither blockade of the metabotropic glutamate receptors nor of the NMDA receptor significantly influenced the three types of spontaneous EA. Only the non-NMDA antagonist CNQX completely and reversibly blocked the generation and propagation of EA in the neonatal IHF, suggesting that as in the juvenile (P10–24, Avoli *et al*., 1993) and adult (Avoli *et al*., 1996) rat hippocampus, AMPA receptors are essential for the generation of EA. Therefore, in spite of the low density of glutamatergic synapses at an early developmental stage, synchronized ictal and interictal activities can be generated and persisted for long periods. Recent studies also suggest that repeated episodes of EA generate a mirror focus and other alterations in synaptic activities in the neonatal circuit *in vitro* (Khalilov *et al*., 1997, 1999). Future studies will have to determine whether these effects are due to an EA-induced acceleration of the expression of glutamatergic receptors.

Acknowledgements

This work was supported by grants of the Deutsche Forschungsgemeinschaft to H.J.L. (Lu 375/3-2 and 3-3) and of the INSERM to Y.B.-A. and V.I.D.

Abbreviations

4-AP, 4-aminopyridine; ACSF, artificial cerebrospinal fluid; AMPA, α-amino-3-hydroxy-5-methyl-4-isoxazolepropionic; APV, DL-2-amino-5-phosphonovaleric acid; CNQX, 6-cyano-7-nitroquinoxaline-2,3-dione; EA, epileptiform activity; EGTA, ethylene glycol-bis (b-aminoethyl ether)-*N*,*N*,*N*′,*N*′-tetraacetic acid; GABA, γ-aminobutyric acid; GDP, giant depolarizing potential; HEPES, *N*-2-hydroxyethylpiperazine-*N*-2-ethanesulphonic acid; IHF, intact hippocampal formation; MCPG, (±)-alpha-methyl-4-carboxyphenylglycine; MK-801, (+)-MK-801 hydrogen maleate; NMDA, *N*-methyl-D-aspartate; P, postnatal day.

References

Aicardi, J. (1986) *Epilepsy in Children*. Raven Press, New York.

Avoli, M., Barbarosie, M., Lücke, A., Nagao, T., Lopantsev, V. & Köhling, R. (1996) Synchronous GABA-mediated potentials and epileptiform discharges in the rat limbic system *in vitro*. *J. Neurosci.*, **16**, 3912–3924.

Avoli, M., Psarropoulou, C., Tancredi, V. & Fueta, Y. (1993) On the synchronous activity induced by 4-aminopyridine in the CA3 subfield of juvenile rat hippocampus. *J. Neurophysiol.*, **70**, 1018–1029.

Barbarosie, M. & Avoli, M. (1997) CA3-driven hippocampal-entorhinal loop controls rather than sustains *in vitro* limbic seizures. *J. Neurosci.*, **17**, 9308–9314.

Bayer, S.A. (1980) Development of the hippocampal region in the rat. I. Neurogenesis examined with 3H-thymidine autoradiography. *J. Comp. Neurol.*, **190**, 87–114.

Ben-Ari, Y. (1987) Brain damage caused by seizure activity. *Electroencephalogr. Clin. Neurophysiol. Suppl.*, **39**, 209–211.

Ben-Ari, Y., Cherubini, E., Corradetti, R. & Gaiarsa, J.-L. (1989) Giant synaptic potentials in immature rat CA3 hippocampal neurones. *J. Physiol.* (*Lond.*), **416**, 303–325.

Ben-Ari, Y., Khazipov, R., Leinekugel, X., Caillard, O. & Gaiarsa, J.L. (1997) $GABA_A$, NMDA and AMPA receptors: a developmentally regulated 'menage a trois'. *Trends Neurosci.*, **20**, 523–529.

Cherubini, E., De Feo, M.R., Mecarelli, O. & Ricci, G.F. (1983) Behavioral and electrographic patterns induced by systemic administration of kainic acid in developing rats. *Brain Res.*, **285**, 69–77.

Diabira, D., Hennou, S., Chevassus-Au-Louis, N., Ben Ari, Y. & Gozlan, H. (1999) Late embryonic expression of AMPA receptor function in the CA1 region of the intact hippocampus in vitro. *Eur. J. Neurosci.*, **11**, 4015–4023.

Durand, G.M., Kovalchuk, Y. & Konnerth, A. (1996) Long-term potentiation and functional synapse induction in developing hippocampus. *Nature*, **381**, 71–75.

Gomez-Di Cesare, C.M., Smith, K.L., Rice, F.L. & Swann, J.W. (1997) Axonal remodeling during postnatal maturation of CA3 hippocampal pyramidal neurons. *J. Comp. Neurol.*, **384**, 165–180.

Heinemann, U., Zhang, C.L. & Eder, C. (1993) Entorhinal cortex–hippocampal interactions in normal and epileptic temporal lobe. *Hippocampus*, **3** (Suppl.), 89–98.

Holmes, G.L. & Ben-Ari, Y. (1998) Seizures in the developing brain: perhaps not so benign after all. *Neuron*, **21**, 1231–1234.

Iijima, T., Witter, M.P., Ichikawa, M., Tominaga, T., Kajiwara, R. & Matsumoto, G. (1996) Entorhinal–hippocampal interactions revealed by real-time imaging. *Science*, **272**, 1176–1179.

Isaac, J.T.R., Nicoll, R.A. & Malenka, R.C. (1995) Evidence for silent synapses: implications for the expression of LTP. *Neuron*, **15**, 427–434.

Jones, R.S.G. (1993) Entorhinal-hippocampal connections: a speculative view of their function. *Trends Neurosci.*, **16**, 58–64.

Katz, L.C. (1993) Coordinate activity in retinal and cortical development. *Curr. Opin. Neurobiol.*, **3**, 93–99.

Khalilov, I., Dzhala, V., Medina, I., Leinekugel, X., Melyan, Z., Lamsa, K., Khazipov, R. & Ben-Ari, Y. (1999) Maturation of kainate-induced epileptiform activities in interconnected intact neonatal limbic structures in vitro. *Eur. J. Neurosci.*, **11**, 3468–3480.

Khalilov, I., Esclapez, M., Medina, I., Aggoun, D., Lamsa, K., Leinekugle, X., Khazipov, R. & Ben-Ari, Y. (1997) A novel in vitro preparation: the intact hippocampal formation. *Neuron*, **19**, 743–749.

Khazipov, R., Leinekugel, X., Khalilov, I., Gaiarsa, J.L. & Ben-Ari, Y. (1997) Synchronization of GABAergic interneuronal network in CA3 subfield of neonatal rat hippocampal slices. *J. Physiol.* (*Lond.*), **498**, 763–772.

Lee, P.H., Xie, C.W., Lewis, D.V., Wilson, W.A., Mitchell, C.L. & Hong, J.S. (1990) Opioid-induced epileptiform bursting in hippocampal slices: higher susceptibility in ventral than dorsal hippocampus. *J. Pharmacol. Exp. Ther.*, **253**, 545–551.

Leinekugel, X., Khalilov, I., Ben Ari, Y. & Khazipov, R. (1998) Giant depolarizing potentials: the septal pole of the hippocampus paces the activity of the developing intact septohippocampal complex in vitro. *J. Neurosci.*, **18**, 6349–6357.

Linke, R. & Frotscher, M. (1993) Development of the rat septohippocampal projection: tracing with DiI and electron microscopy of identified growth cones. *J. Comp. Neurol.*, **332**, 69–88.

Lothman, E.W. (1994) Seizure circuits in the hippocampus and associated structures. *Hippocampus*, **4**, 286–290.

Lothman, E.W., Bertram, E.H. III & Stringer, J.L. (1991) Functional anatomy of hippocampal seizures. *Prog. Neurobiol.*, **37**, 1–82.

Luhmann, H.J., Reiprich, R.A., Haul, S., Leinekugel, X. & Ben-Ari, Y. (1998) 4-Aminopyridine induced epileptiform activity in the intact neonatal rat hippocampal formation in vitro. *Soc. Neurosci. Abstr.*, **14**, 1935.

Morest, D.K. (1970) A study of neurogenesis in the forebrain of opossum pouch young. *Z. Anat. Entwicklungsgesch.*, **130**, 265–305.

Nitecka, L., Tremblay, E., Charton, G., Bouillot, J.P., Berger, M.L. & Ben-Ari, Y. (1984) Maturation of kainic acid seizure–brain damage syndrome in the rat. II. Histopathological sequelae. *Neuroscience*, **13**, 1073–1094.

Palva, J.M., Lamsa, K., Lauri, S.E., Rauvala, H., Kaila, K. & Taira, T. (2000)

Fast network oscillations in the newborn rat hippocampus in vitro. *J. Neurosci.*, **20**, 1170–1178.
Paré, D., DeCurtis, M. & Llinás, R.R. (1992) Role of the hippocampal-entorhinal loop in temporal lobe epilepsy: extra- and intracellular study in the isolated guinea pig brain *in vitro*. *J. Neurosci.*, **12**, 1867–1881.
Perreault, P. & Avoli, M. (1989) Effects of low concentrations of 4-amino-pyridine on CA1 pyramidal cells of the hippocampus. *J. Neurophysiol.*, **61**, 953–970.
Schwartzkroin, P.A. & Prince, D.A. (1978) Cellular and field potential properties of epileptogenic hippocampal slices. *Brain Res.*, **147**, 117–130.
Supèr, H. & Soriano, E. (1994) The organization of the embryonic and early postnatal murine hippocampus. II. Development of entorhinal, commissural, and septal connections studied with the lipophilic tracer DiI. *J. Comp. Neurol.*, **344**, 101–120.
Swann, J.W. & Brady, R.J. (1984) Penicillin-induced epileptogenesis in immature rat CA3 hippocampal pyramidal cells. *Dev. Brain Res.*, **12**, 243–254.
Swanson, L.W. & Cowan, W.M. (1977) An autoradiographic study of the organization of the efferent connections of the hippocampal formation in the rat. *J. Comp. Neurol.*, **172**, 49–84.
Tremblay, E., Nitecka, L., Berger, M.L. & Ben-Ari, Y. (1984) Maturation of kainic acid seizure–brain damage syndrome in the rat. I. Clinical, electrographic and metabolic observations. *Neuroscience*, **13**, 1051–1072.
Tyzio, R., Represa, A., Jorquera, I., Ben-Ari, Y., Gozlan, H. & Aniksztejn, L. (1999) The establishment of GABAergic and glutamatergic synapses on CA1 pyramidal neurons is sequential and correlates with the development of the apical dendrite. *J. Neurosci.*, **19**, 10 372–10 382.
Witter, M.P. (1993) Organization of the entorhinal-hippocampal system: a review of current anatomical data. *Hippocampus*, **3** (Suppl.), 33–44.